Compact Colorless Tunable Dispersion Compensator With 1000-ps/nm Tuning Range for 40-Gb/s Data Rates

Dan M. Marom, *Member, IEEE*, Christopher R. Doerr, *Member, IEEE*, Mark A. Cappuzzo, Evans Yifan Chen, A. Wong-Foy, L. T. Gomez, and S. Chandrasekhar, *Fellow, IEEE*

***Abstract*—A novel tunable dispersion compensator (TDC) with ±500-ps/nm tuning range and bandwidth support for 40-Gb/s signals is described. The TDC is constructed from a waveguide grating router (WGR) that provides very high spatial dispersion and a deformable cylindrical mirror for applying quadratic spatial phase across the dispersed wavefront. The WGR's 100-GHz free-spectral range (FSR) allows the device to simultaneously apply the same dispersion to all wavelength-division multiplexing (WDM) channels.**

***Index Terms*—Dispersion compensation, gratings, microelectromechanical devices, microelectromechanical system (MEMS), optical filters.**

I. Introduction

AN OPTICAL tunable dispersion compensator (TDC) is an essential component for 40-Gb/s long-reach communication links. Fiber temperature changes in long links are sufficient to require the use of a TDC, and electronic dispersion compensation at 40 Gb/s is currently too immature. Oftentimes, the TDC needs to be colorless—having a free-spectral range (FSR) equal to the channel spacing—enabling reconfigurable wavelength-division multiplexing (WDM) networks and reducing inventory. Bulk-optic [1]–[4], ring-resonator [5], waveguide-grating-router (WGR) [6], sampled chirped fiber Bragg gratings [7], and Mach–Zehnder-interferometer [8], [9] colorless TDCs have been demonstrated. Other desirable TDC features include fast tuning speed, single-knob dispersion adjustment, low power consumption, and small size.

The WGR-based TDC is colorless, bandwidth efficient, and compact; has fast tuning and single-knob adjustment; and can provide a very large tuning range. Recently, we presented a WGR-based TDC that uses a deformable mirror [10] rather than a thermooptic lens [6], saving significant power consumption and size. In this paper, we provide further design details and measurement results. We note that a non-tunable dispersion compensator using a WGR and a fixed mirror was previously demonstrated [11]. Our WGR has an extremely high spectral resolution; and with it, we demonstrate 1000-ps/nm tuning range, which is the largest reported for a 40-Gb/s 100-GHz-FSR TDC to our knowledge. A 40-Gb/s TDC with 1600-ps/nm tuning range is presented in [12], but it had a 200-GHz FSR, requiring two codes to cover all WDM channels. Our project is also the first demonstration of a polarization-independent WGR-based TDC without using polarization diversity.

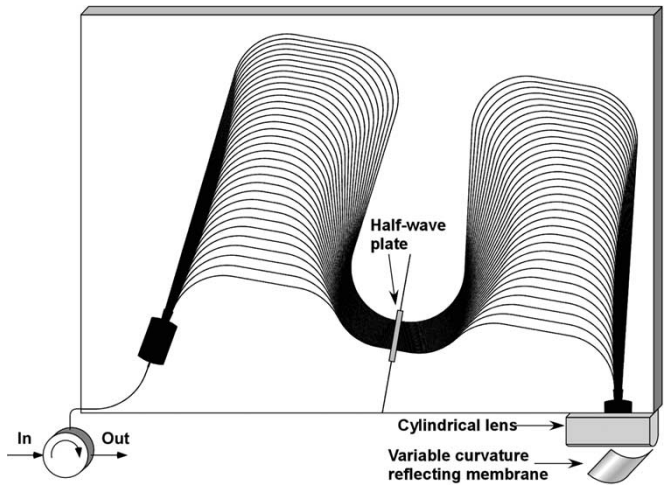

Fig. 1. Schematic layout of the optical TDC, comprising of a WGR, collimation lens, deformable mirror, and a circulator.

II. Design of TDC

The waveguide layout and the concept of the TDC are shown in Fig. 1. Light enters a planar lightwave circuit (PLC) containing an extremely high-resolution WGR through the single waveguide that is attached to an optical circulator, which is used to separate the input and output signal. The light passes through a first free-space region in the PLC, is coupled into the WGR, and enters a second free-space region. At this second free-space region, the PLC is cut and the light is then spectrally spread out across a variable-curvature reflecting membrane. There is a plano-cylindrical glass lens attached to the PLC that collimates the light in the plane of the PLC. To achieve linear chromatic dispersion, one must apply a phase distribution that varies quadratically with wavelength. Fig. 2 illustrates the effects of cutting the free-space region and of the variable-curvature reflecting mirror. The free-space region in a conventional PLC

Manuscript received July 20, 2005; revised October 25, 2005.

D. M. Marom was with Bell Laboratories, Lucent Technologies, Holmdel, NJ 07733 USA. He is now with the School of Computer Science and Engineering, Hebrew University, Jerusalem, Israel (e-mail: dmarom@lucent.com).

C. R. Doerr, and S. Chandrasekhar are with Bell Laboratories, Lucent Technologies, Holmdel, NJ 07733 USA.

M. A. Cappuzzo, E. Y. Chen, A. Wong-Foy, and L. T. Gomez are with Bell Laboratories, Murray Hill, NJ 07974 USA.

Digital Object Identifier 10.1109/JLT.2005.861137

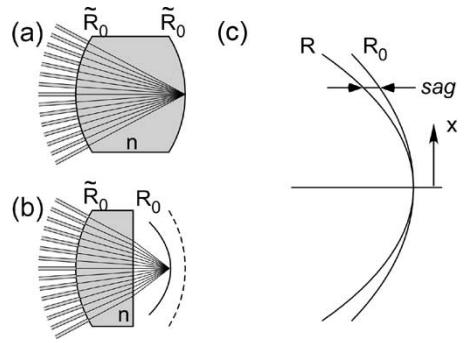

Fig. 2. (a) Free-space region as normally implemented inside a PLC. (b) Free-space region is cut and light propagates in air. The zero-dispersion curvature and location of the second surface of free-space region changes in air. (c) Adjusting the surface curvature of the membrane results in spatially varying sag values, which are approximately quadratic.

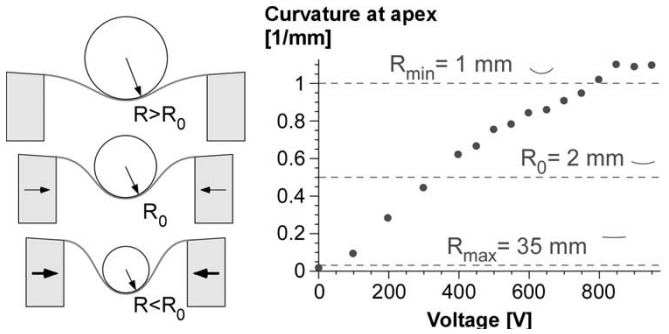

Fig. 3. (Left) Reflecting membrane stretched between two actuators. As the actuators move towards each other, the membrane buckles resulting in a curved region at the center. (Right) Measured curvature versus applied voltage on the piezoelectric actuators.

design consists of two curved surfaces of radii $\tilde{R}_0$ (the tilde overscript denotes properties in the guided medium), where the center of curvature of one surface lies on the second surface. In this work, we cut through the free-space region and allow the light to radiate into air. The radius of curvature of the second surface R_0 is decreased to $\tilde{R}_0/n$, where n is the refractive index of the PLC guiding material to account for refraction at the interface, and the propagation distance to the second surface decreases as a function of the cut location. As the second surface of the free-space region is now in air, its curvature may be dynamically adjusted to differ from R_0. The membrane sag, which we define as the propagation-direction distance between the adjusted membrane radius of curvature R and the zero-dispersion radius of curvature R_0, as a function of the distance from the origin x is well approximated by

$$\mathrm{sag}(R,x) = \frac{x^2(R-R_0)}{2R\cdot R_0}. \tag{1}$$

The reflection of spatially dispersed light from the membrane's quadratic phase distribution produces a chromatic dispersion, which is given by

$$D = -\frac{2\lambda_0}{c_0}\left(\frac{R-R_0}{R\cdot R_0}\right)\left(\frac{dx}{d\lambda}\right)^2 \tag{2}$$

where λ_0 is the free-space wavelength, c_0 is the free-space speed of light, and $dx/d\lambda$ is the spatial dispersion defined by the WGR parameters

$$\frac{dx}{d\lambda} = \frac{c_0\tilde{R}_0}{na\Delta f\lambda_0} \tag{3}$$

where a is the grating-arm pitch at the first curved surface of the free-space region, and Δf is the WGR FSR. In our case, $\tilde{R}_0 = 3.0$ mm, $a = 11.5$ μm, and $\Delta f = 100$ GHz. Therefore, the zero-dispersion curvature of the adjustable membrane is $R_0 = 2$ mm, and chromatic dispersion values of ± 500 ps/nm can be achieved for $R = 1$ mm and $R = 35$ mm, respectively.

In our chosen optical design parameters, the curvature of the reflecting membrane does not have to change its sign (e.g., transition from concave to convex) within the desired dispersion tuning range. This allows us to use the buckling mode of the membrane for changing its curvature and always remain buckled in the same direction (see Fig. 3). The reflecting membrane is stretched across two inward-propagating actuators at a large initial radius of curvature. As the two actuators are activated, the membrane ends are brought closer to each other and the radius of curvature decreases. We cut a strip of 2-mil-thick aluminum-coated Mylar [13], which is 2.5-mm wide, and glued its ends to two piezo-electric actuators, each with a 30-μm achievable displacement. Compressive springs were inserted between the two actuators to tension the arrangement. The membrane-buckling technique allows us to achieve large curvature variations for very small end displacements. The membrane curvatures were characterized with an interferometric profilometer. The central 200 μm of the membrane exhibited a very good fit to a quadratic sag profile, as required for the TDC operation. One limitation of the membrane-buckling approach is that the membrane center (or apex) translates as a function of the end displacement, as opposed to a desired change of curvature about a stationary apex, as depicted in Fig. 2. Using a cosine profile model for the buckled-membrane contour (with the two edges rigidly supported), we calculate that the apex translates by ± 100 μm at the ± 500-ps/nm TDC settings, respectively.

In our PLC layout (Fig. 1), the WGR is "pinched" in the middle [14]. The pinching results in 1) significant savings in consumed wafer area; 2) significant reduction of the grating sensitivity to refractive-index gradients in the wafer by occupying a smaller extent; and 3) enabling the insertion of a small half-wave plate to make the TDC polarization independent (the WGR is perfectly symmetric about its center line). Despite the pinching, such a high-resolution WGR is still expected to have significant fabrication-induced phase errors. The phase errors can be divided into linear, quadratic, and higher order distributions across the grating arms. One significant advantage of our design is that the linear component is compensated by adjusting the WGR temperature, and the quadratic component is compensated by adjusting the focal position of the deformable mirror when the device is assembled.

III. Results

The silica-on-silicon WGR was fabricated with 0.8%-index-contrast waveguides and has 34 grating arms. We took the silica waveguide chip with the WGR, cut a slot in it, inserted the

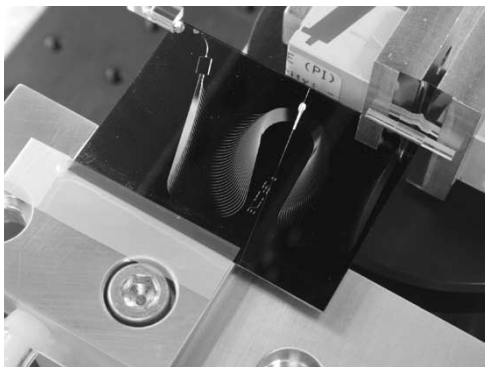

Fig. 4. Photograph of TDC showing the PLC, the attached cylindrical collimation lens, and the deformable Mylar mirror next to lens. The physical size of the PLC is 30 mm $\times$ 50 mm.

zero-order waveplate, glued on the input/output fiber, attached it to a circulator, and glued on the plano-cylindrical lens. The deformable-mirror assembly was aligned with respect to the WGR (Fig. 4). Since there are only two elements (WGR and deformable membrane) that need to be aligned with respect to each other, this step is straightforward. The other diffraction orders from the WGR were extinguished by placing an aperture (baffles, not shown in Fig. 4) near the mirror plane. Both piezoelectric actuators were wired in parallel, so only one voltage knob was required to adjust the dispersion.

The TDC demonstrated more than $\pm$500-ps/nm tuning range (Fig. 5(top)), which is obtained for applied actuator voltages between 100 V (negative dispersion) to 800 V (positive dispersion). The insertion loss, including the circulator, was $\sim$ 8 dB at the zero dispersion setting and increased to $\sim$ 11–12 dB at the $\pm$500-ps/nm settings. Our calculations show that the effect of defocusing, due to the translation of the membrane apex by 100 μm (violating the confocal arrangement), contributes $\sim$ 3-dB excess loss. At the extreme tuning positions, the transmissivity passband exhibited narrowing [Fig. 5(center)] because the mirror deflects the spectral components at the passband extremes further away from the center of the star coupler. The group delay ripple (GDR) was less than $\pm$6 ps over 70-GHz of bandwidth, for support of 40-Gb/s transmission rates [Fig. 5(bottom)]. The polarization-dependent loss (PDL) across the central 70-GHz bandwidth ranged from 0.5 dB at 0 ps/nm to 3.5 dB at the tuning extremes. Likewise, the worst case differential group delay (DGD) varied from $<$ 1 ps at 0 ps/nm to $<$ 7 ps at the tuning extremes. The Mylar film contributed to some of the polarization performance degradations; testing with a fixed parabolic gold-coated mirror exhibited low PDL and DGD.

The dispersion-compensation capability of the TDC was tested using a 42.7-Gb/s carrier-suppressed return-to-zero (CSRZ) $2^{31}-1$ pseudorandom bit sequence at 1550 nm, with different spools of fibers [single-mode fiber (SMF) and dispersion-compensating fiber (DCF)] placed between the transmitter and the receiver to generate various dispersion values [Fig. 6(a)]. CSRZ is a stringent test of a TDC because of its wide bandwidth. At the receiver, a wavelength demultiplexer preceded the TDC, which is followed by an optical preamplifier and a p-i-n photodetector into a 40-Gb/s electrical

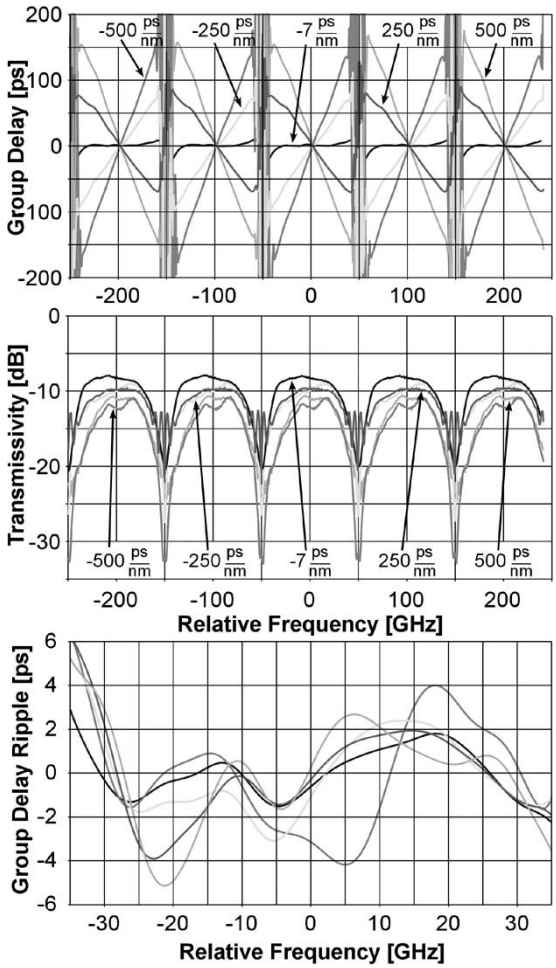

Fig. 5. (Top) Group delay versus frequency. Different slopes are observed, corresponding to dispersion settings. (Center) TDC transmissivity versus frequency. Spectral narrowing is observed for larger departures from zero dispersion. Passband and dispersion settings are repeated at 100-GHz FSR. (Bottom) GDR for all dispersion settings at one particular channel. Ripple is bounded by $\pm$6 ps over $\pm$35 GHz from channel center.

demultiplexer. No polarization control was allowed. Tuning the TDC was trivial, as a single knob operation yielded immediate eye opening at the proper setting [Fig. 6(b)–(g)]. At the 0-ps/nm setting, the TDC showed zero penalty in bit-error rate (BER) versus optical signal-to-noise ratio (OSNR) over the back-to-back case [Fig. 7(top)]. Penalty at the dispersion extremes of $\pm$500 ps/nm was $\sim$ 1-dB OSNR at 10^{-3} BER and $\sim$ 3-dB OSNR at 10^{-9} BER. We attribute the greater penalty with negative dispersion (as the Mylar film flattens) to the passband narrowing, as the GDR is well behaved throughout the tuning range. Sensitivity to channel misalignment was tested by detuning the laser line with respect to the channel center frequency [Fig. 7(bottom)], yielding a $\sim$ 1-dB OSNR penalty at 10^{-9} BER with 2.5-GHz detuning.

The TDC time responses were measured by driving the piezoelectric actuators with a square wave voltage and tracking the BER counts on an oscilloscope (Fig. 8). The TDC-dispersion increase (actuate) and decrease (restore) times were $\sim$ 200 μs and $\sim$ 20 ms, respectively. The time to decrease the dispersion (flatten the mirror) is significantly slower and exhibits two time constants. We believe that the slower time

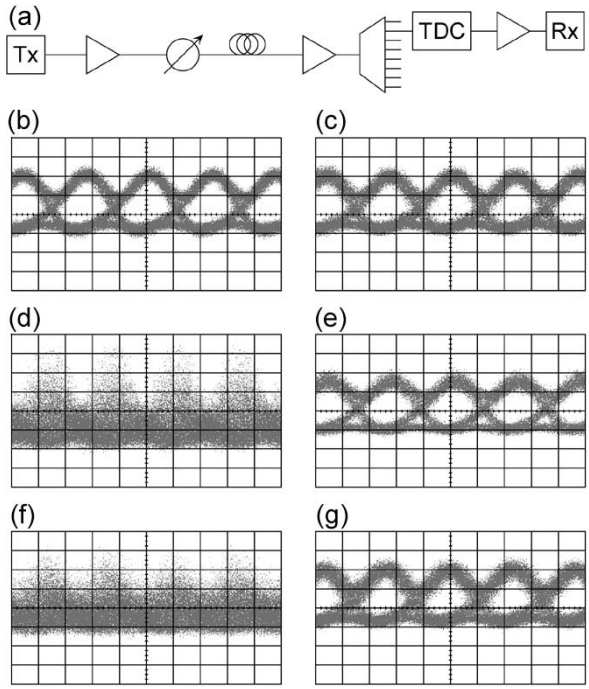

Fig. 6. (a) Setup for characterization of TDC performance in receiver sensitivity experiments. (b) Back-to-back performance of transmitter and receiver. (c) TDC inserted in a transmission link. (d) SMF inserted, generating 425-ps/nm dispersion. (e) TDC compensating 425-ps/nm dispersion. (f) DCF inserted, generating −504-ps/nm dispersion. (g) TDC compensating −504-ps/nm dispersion.

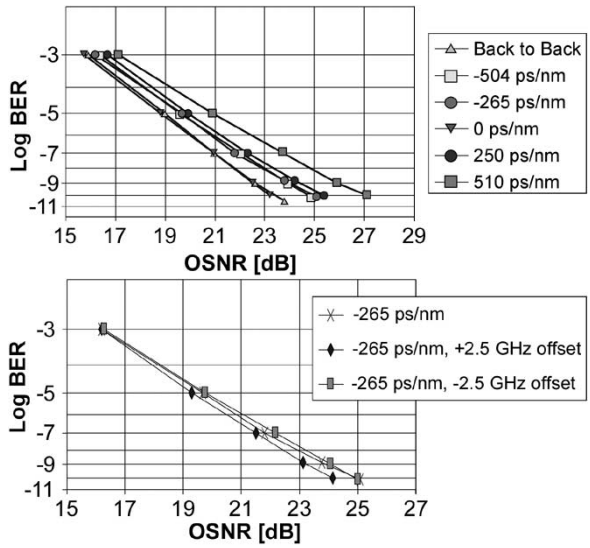

Fig. 7. (Top) Receiver sensitivity curves for different amounts of fiber dispersion in the link. The legend dispersion values are of the inserted fiber, and the TDC dispersion setting is the opposite of that. (Bottom) Sensitivity curves for laser transmitter misalignment with respect to filter center.

constant in the membrane flattening might be due to a Mylar stress relaxation process. Additionally, open loop operation of piezoelectric actuators is known to exhibit both hysteresis and creep behavior, which might also account for the slower relaxation time constant. While 20 ms is significantly faster than some TDC technologies, such as chirped fiber Bragg gratings and mechanical mirror translation in the virtually imaged phased array, it may be too slow for protection switching in reconfigurable networks.

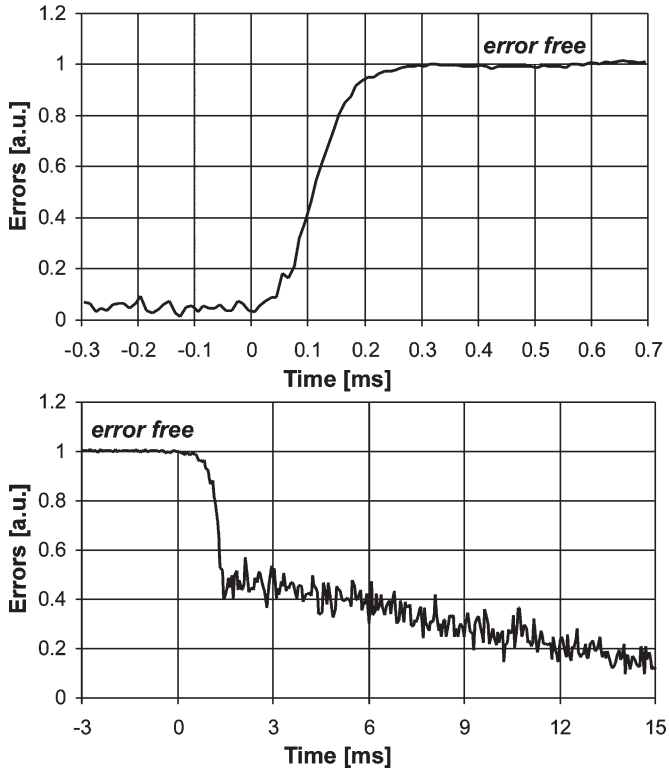

Fig. 8. TDC response time measurements performed with receiver error counts. (Top) Fast response to increasing voltage (dispersion). (Bottom) Slower response to decreasing voltage (dispersion) with two time constants visible.

IV. Conclusion

We demonstrated a novel TDC that combines guided wave optics within a PLC and free-space optics, as well as mechanical optics, to achieve a large tuning range with single-knob tuning, a small size, fast adjustment, low power consumption, and an FSR that matches the usual channel spacing for 40-Gb/s systems. Further improvements to the deformable actuator are expected to further improve the performance (reducing insertion losses, GDR, PDL, and DGD). The actuation mechanism should ensure that the membrane apex does not translate as a function of curvature, as in the case of our buckling membrane approach. One possible improved implementation might consist of a microelectromechanical system (MEMS)-based actuator, which might integrate additional rotational and translational functionality to further facilitate assembly and alignment. Moreover, MEMS-based devices can also be designed to provide the faster actuation speeds that might be required in optical networks (eliminating the slow time constant that we experienced when flattening the membrane).

References

[1] M. Shirasaki, "Chromatic dispersion compensator using virtually imaged phased array," *IEEE Photon. Technol. Lett.*, vol. 9, no. 12, pp. 1598–1600, Dec. 1997.

[2] F. Gires and P. Tournois, "An interferometer useful for pulse compression of a frequency modulated light pulse," *C. R. Acad. Sci.*, vol. 258, pp. 6112–6115, 1964.

[3] C. K. Madsen and J. H. Zhao, *Optical Filter Design and Analysis: A Signal Processing Approach*. New York: Wiley.
[4] D. J. Moss, S. McLaughlin, G. Randall, M. Lamont, M. Ardekani, P. Colbourne, S. Kiran, and C. A. Hulse, "Multichannel tunable dispersion compensation using all-pass multicavity etalons," in *Optical Fiber Communication Conf.*, Anaheim, CA, 2002, vol. 1, pp. 162–163.
[5] C. K. Madsen, G. Lenz, A. J. Bruce, M. A. Cappuzzo, L. T. Gomez, and R. E. Scotti, "Integrated all-pass filters for tunable dispersion and dispersion slope compensation," *IEEE Photon. Technol. Lett*, vol. 11, no. 12, pp. 1623–1625, Dec. 1999.
[6] C. R. Doerr, L. W. Stulz, S. Chandrasekhar, and R. Pafchek, "Colorless tunable dispersion compensator with 400-ps/nm range integrated with a tunable noise filter," *IEEE Photon. Technol. Lett.*, vol. 15, no. 9, pp. 1258–1260, Sep. 2003.
[7] J.-X. Cai, K.-M. Feng, A. E. Willner, V. Grubsky, D. S. Starodubov, and J. Feinberg, "Simultaneous tunable dispersion compensation of many WDM channels using a sampled nonlinearity chirped fiber Bragg grating," *IEEE Photon. Technol. Lett.*, vol. 11, no. 11, pp. 1455–1457, Nov. 1999.
[8] K. Takiguchi, K. Jinguji, K. Okamoto, and Y. Ohmori, "Variable group-delay dispersion equalizer using lattice-form programmable optical filter on planar lightwave circuit," *IEEE J. Sel. Topics Quantum Electron.*, vol. 2, no. 2, pp. 270–276, Jun. 1996.
[9] M. Bohn, F. Horst, B. J. Offrein, G. L. Bona, E. Meissner, and W. Rosenkranz, "Tunable dispersion compensation in a 40 Gb/s system using a compact FIR lattice filter in SiON technology," presented at the Eur. Conf. Optical Communication, Copenhagen, Denmark, 2002, Paper 4.2.3.
[10] C. R. Doerr, D. M. Marom, M. A. Cappuzzo, E. Y. Chen, A. Wong-Foy, L. T. Gomez, and S. Chandrasekhar, "40-Gb/s colorless tunable dispersion compensator with 1000-ps/nm tuning range employing a planar lightwave circuit and a deformable mirror," in *Proc. Optical Fiber Communication (OFC)*, Anaheim, CA, 2005, vol. 6, pp. 13–15. PD.
[11] H. Tsuda, K. Okamoto, T. Ishii, K. Naganuma, Y. Inoue, H. Takenouchi, and T. Kurokawa, "Second- and third-order dispersion compensator using a high-resolution arrayed-waveguide grating," *IEEE Photon. Technol. Lett.*, vol. 11, no. 5, pp. 569–571, May 1999.
[12] H. Ooi, K. Nakamura, Y. Akiyama, T. Takahara, T. Terahara, Y. Kawahata, H. Isono, and G. Ishikawa, "40-Gb/s WDM transmission with virtually imaged phased array (VIPA) variable dispersion compensators," *J. Lightw. Technol.*, vol. 20, no. 12, pp. 2196–2203, Dec. 2002.
[13] *Mylar Film Courtesy of Grafix Plastics*, Cleveland, OH. [Online]. Available: http://www.grafixplastics.com/
[14] K. Takada, M. Abe, T. Shibata, and K. Okamoto, "1-GHz-spaced 16-channel arrayed-waveguide grating for a wavelength reference standard in DWDM network systems," *J. Lightw. Technol.*, vol. 20, no. 5, pp. 850–853, May 2002.

Dan M. Marom (S'97–M'00) received the B.Sc. degree in mechanical engineering in 1989 and the M.Sc. degree in electrical engineering in 1995, both from Tel-Aviv University, Tel-Aviv, Israel, and the Ph.D. degree in electrical engineering in 2000 from the University of California at San Diego (UCSD), La Jolla. In his doctoral dissertation, he investigated femtosecond-rate optical signal processing with applications in ultrafast communications.

From 1996 through 2000, he was a Fannie and John Hertz Foundation Graduate Fellow at UCSD. From 2000 to 2005, he was a member of Technical Staff at the Advanced Photonics Research Department of Bell Laboratories, Lucent Technologies, Holmdel, NJ, where his activity focused on novel photonic devices utilizing MEMS, PLC, and free-space technologies for optical communications. In 2005, he joined the faculty of the School of Computer Science and Engineering, Hebrew University, Jerusalem, Israel.

Dr. Marom received the IEEE Lasers and Electro-Optics Society Best Student Paper Award in 1999 for his work describing instantaneous time reversal of complex amplitude ultrafast waveforms.

Christopher R. Doerr (M'95) received the B.S. degree in aeronautical/astronautical engineering in 1989 and the B.S. and M.S. degrees in 1990 and the Ph.D. degree in 1995 in electrical engineering, all from the Massachusetts Institute of Technology (MIT), Cambridge. He attended MIT on an Air Force ROTC scholarship and earned his pilot wings at Williams AFB, AZ, in 1991. His Ph.D. thesis, on constructing a fiber-optic gyroscope with noise below the quantum limit, was supervised by Prof. H. Haus.

Since coming to Bell Labs, Holmdel, NJ, in 1995, his research has focused on integrated devices for optical communication. He was promoted to Distinguished member of Technical Staff in 2000.

Dr. Doerr received the OSA Engineering Excellence Award in 2002. He is an Associate Editor for the IEEE PHOTONICS TECHNOLOGY LETTERS, is an elected member of the LEOS Board of Governors, and was a subcommittee chair for OFC 2005.

Mark A. Cappuzzo received the B.A. degree from Rutgers University, New Brunswick, NJ, in 1979 and the M.S. degree from Fairleigh Dickinson University, Teaneck, NJ, in 1982, both in physics.

After seven years as Adjunct Professor of physics at Rutgers University, he joined Bell Labs at Lucent Technologies, Murray Hill, NJ, in 1987, where he currently is a member of the Technical Staff, working on advanced photolithography techniques and on advanced process integration for the fabrication of planar and hybrid lightwave circuits.

Evans Yifan Chen received the B.S. degree from the Shanghai JiaoTong University, Shanghai, China, in 1994 and the Ph.D. degree from Tohoku University, Sendai, Japan, in 2001, both in applied physics.

While at Tohoku University, he developed molecular beam epitaxy for zinc oxide and investigated its lasing mechanism. He joined Bell Laboratories of Lucent Technologies, Murray Hill, NJ, in 2001, where he is currently working on integrated photonics.

A. Wong-Foy, photograph and biography not available at the time of publication.

L. T. Gomez, photograph and biography not available at the time of publication.

S. Chandrasekhar (F'05) received the B.Sc., M.Sc., and Ph.D. degrees in physics from the University of Bombay, Bombay, India, in 1973, 1975, and 1985, respectively.

He was with the Tata Institute of Fundamental Research, Bombay, from 1975 to 1985 and has been with AT&T Bell Laboratories (now called Bell Laboratories, Lucent Technologies), Crawford Hill Laboratory, Holmdel, NJ, since 1986. He worked on compound semiconductor devices and high-speed optoelectronic integrated circuits (OEICs). Since January 1999, he has been responsible for forward-looking research in WDM optical networking. His current interests include 40-Gb/s transport and networking, modulation formats, and electronic signal processing at the receiver. He is a DMTS at Bell Labs.

Dr. Chandrasekhar is a member of the IEEE Lasers and Electro-Optics Society and an Associate Editor of the IEEE PHOTONICS TECHNOLOGY LETTERS. He has been member of the technical program committees of the IEDM, the DRC, and the OFC conferences. He holds 14 U.S. patents. He received the IEEE LEOS Engineering Achievement Award for 2000 and the OSA Engineering Excellence Award for 2004 for his contributions to OEICs and WDM systems research.